Available online www.jocpr.com

Journal of Chemical and Pharmaceutical Research, 2016, 8(2):86-98

Research Article

ISSN : 0975-7384
CODEN(USA) : JCPRC5

Trigonella stellate extract as corrosion inhibitor for copper in 1M nitric acid solution

A. S. Fouda[*1], A. E. Mohamed[2] and M. A. Khalid[1]

[1]*Department of Chemistry, Faculty of Science, El-Mansoura University, El-Mansoura, Egypt*
[2]*Chemistry Department, Faculty of Science, Suez Canal University, Ismailia, Egypt*

ABSTRACT

The inhibitive effect of Trigonella stellate extract against the corrosion of copper in 1M HNO_3 solution has been investigated using weight loss, potentiodynamic polarization, electrochemical impedance spectroscopy (EIS) and electrochemical frequency modulation (EFM) techniques. Surface morphology was tested using scanning electron microscope (SEM). The effect of the temperature on corrosion behavior of copper in 1 M HNO_3 solution with and without the extract was studied in the temperature range of 25-45^oC by weight loss method. Polarization curves revealed that the investigated extract acts as mixed type inhibitor. The inhibition efficiency was found to increase with the increase in the extract concentration and decrease with raising solution temperature. The adsorption of the inhibitor on copper surface was found to obey Timken's adsorption isotherm. The results obtained from different techniques are in good agreement.

Key words: Corrosion inhibition, HNO_3, *Trigonella stellate* extract, copper

---

INTRODUCTION

Copper is a metal that has a wide range of applications due to its good properties. It is used in electronics, for production of wires, sheets, tubes, and also to form alloys. The use of copper corrosion inhibitors in acid solutions is usually to minimize the corrosion of copper during the acid cleaning and descaling. The possibility of the copper corrosion prevention has attracted many researchers so until now numerous possible inhibitors have been investigated [1-3].Most well-known acid inhibitors are organic compounds containing nitrogen , sulfur, and oxygen atoms. Among them, organic inhibitors have many advantages such as high inhibition efficiency and easy production [4-7]. Organic heterocyclic compounds have been used for the corrosion inhibition of copper [8] in different corroding media. Although many of these compounds have high inhibition efficiencies, several have undesirable side effects, even in very small concentrations, due to their toxicity to humans, deleterious environmental effects, and high-cost [9]. Plant extract is low-cost and environmental safe, so the main advantages of using plant extracts as corrosion inhibitors are economic and safe environment. Uptill now, many plant extracts have been used as effective corrosion inhibitors for copper in acidic media, such as: Zenthoxylum alatum [10], Azadirachta Indica [11] caffeine [12] Cannabis [13]. The inhibition performance of plant extract is normally ascribed to the presence of complex organic species, including tannins, alkaloids and nitrogen bases, carbohydrates and proteins as well as hydrolysis products in their composition. These organic compounds usually contain polar functions with nitrogen, sulfur, or oxygen atoms and have triple or conjugated double bonds with aromatic rings in their molecular structures, which are the major adsorption centers.

The present work was designed to study the inhibitory action of *Trigonella stellate* extract for the corrosion of copper in 1 M HNO_3 using chemical and electrochemical techniques.

EXPERIMENTAL SECTION

2.1 Composition of Copper Samples

Chemical composition of the copper samples in weight %

Element	Sn	Ag	Fe	Bi	PP	AA	Cu
Weight%	0.001	0.001	0.01	0.0005	0.002	0.0002	The rest

2.2. Materials and Solutions

Experiments were performed using copper specimens 1cm^{2}as working electrodemounted in Teflon, an epoxy resin was used to fill the space between Teflon and copper electrode. The auxiliary electrode was a platinum sheet (1 cm^2), saturated calomel electrode (SCE) as reference electrode was connected to a conventional electrolytic cell of capacity 100 ml via a bridge with a Luggin capillary, the tip of which was very close to the surface of the working electrode to minimize the IR drop. The aggressive solution used was prepared by dilution of analytical grade 70% HNO_3 with bidistilled water. The stock solution (1000 ppm) of *Trigonella stellate* was used to prepare the desired concentrations by dilution with bidistilled water. The concentration range of *Trigonella stellate* used was 50-500 ppm.The main chemical components of *Trigonella stellate* are saponins, coumarin, fenugreekine, nicotinic acid, phytic acid, scopoletin and trigonelline.

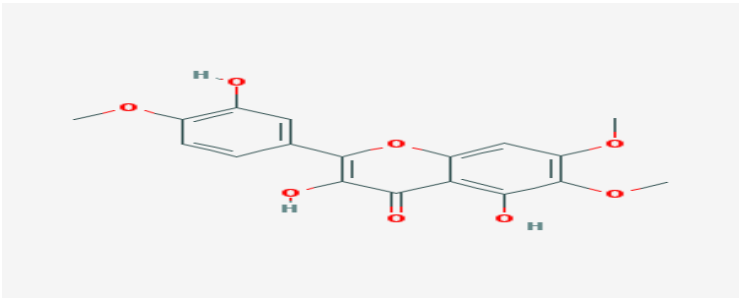

Fig. 1: **Structure of *Trigonella stellate* extract**

2.3 weight Loss Measurements

Seven parallel copper sheets of 2×1.5×0.2 cm were abraded with emery paper (grade 320–500–1200) and then washed with bidistilled water and acetone. After accurate weighing, the specimens were immersed in a 250 ml beaker, which contained 100 ml of HNOwith and without addition of different concentrations of *Trigonella stellate*. All the aggressive acid solutions were open to air. After 180 minutes, the specimens were taken out, washed, dried, and weighed accurately. The average weight loss of seven parallel copper sheets could be obtained. The inhibition efficiency (IE %) and the degree of surface coverage, θ of the extract were calculated as follows [14]:

$$IE\%=\theta\times100= 1- [(W/W°)] \times100 \qquad (1)$$

where W^o and W are the values of the average weight losses without and with addition of the extract, respectively.

2.4. Electrochemical Measurements

All the measurements were done in solutions open to atmosphere under unstirred conditions. All potential values were reported versus SCE. Prior to each experiment, the electrode was treated as before. Tafel polarization curves

were obtained by changing the electrode potential automatically from (-0.8 to 1 V vs. SCE) at open circuit potential with a scan rate of 1 mVs^{-1}. Stern-Geary method [15], used for the determination of corrosion current is performed by extrapolation of anodic and cathodic Tafel lines to a point which gives (log i_{corr}) and the corresponding corrosion potential (E_{corr}) for extract free acid and for each concentration of the extract. Then (i_{corr}) was used for calculation of inhibition efficiency (IE %) and surface coverage (θ) as in equation 2:

$$IE\% = \Theta \times 100 = 1 - [i_{cor(inh)} / i_{(free)}] \times 100 \quad (2)$$

where $i_{corr(free)}$ and $i_{corr(inh)}$ are the corrosion current densities in the absence and presence of the extract, respectively . Impedance measurements were carried out in frequency range ($2x10^4$ Hz to $8x10^{-2}$ Hz) with amplitude of 10 mV peak-to-peak using ac signals at open circuit potential. The experimental impedance was analyzed and interpreted based on the equivalent circuit. The main parameters deduced from the analysis of Nyquist diagram are the charge transfer resistance R_{ct} (diameter of high-frequency loop) and the double layer capacity C_{dl}. The inhibition efficiencies and the surface coverage (θ) obtained from the impedance measurements are calculated from equation 3:

$$IE\% = \Theta \times 100 = 1 - [R_{ct}^{o} / R_{ct}] \times 100 \quad (3)$$

where R^{o}_{ct} and R_{ct} are the charge transfer resistance in the absence and presence of the extract, respectively. Electrochemical frequency modulation (EFM) was carried out using two frequencies 2 and 5 Hz. The higher frequency must be at least two times the lower one. The higher frequency must also be sufficiently slow that the charging of the double layer does not contribute to the current response. Often, 10 Hz is a reasonable limit. The large peaks were used to calculate the corrosion current density (i_{corr}), the Tafel slopes (β_a and β_c) and the causality factors CF-2&CF-3 [16]. The electrode potential was allowed to stabilize 30 min before starting the measurements. All the experiments were conducted at 25°C.

All electrochemical measurements were performed using Gamry Instrument (PCI4/750) Potentiostat. Galvanostat/ZRA. This includes a Gamry framework system based on the ESA400. Gamry applications include DC105 software for potentiodynamic polarization, EIS300 software for electrochemical impedance spectroscopy, and EFM140 software for electrochemical frequency modulation measurements via computer for collecting data. Echem Analyst 6.03 software was used for plotting, graphing, and fitting data. To test the reliability and reproducibility of the measurements, duplicate experiments, which performed in each case at the same conditions.

2.5. Surface Morphology

For morphological study, surface features (1 cm x 1 cm x 0.2cm) of copper were examined before and after exposure to 1 M HNO_3 solutions for 12 hours with and without the extract. JEOL JSM-5500 scanning electron microscope was used for this investigation.

RESULTS AND DISCUSSION

3.1 Weight Loss Tests

Weight loss measurements were carried out for copper in 1 M HNO_3 in the absence and presence of different concentrations of *Trigonella stellate* and are shown in Figure (2). The inhibition efficiency (IE %) values calculated are listed in Tables 1& 2. From these tables, it is noted that the IE% increases steadily with increasing the concentration of the extract and decrease with raising the temperature from 25-45ºC. The inhibition efficiency (IE %) and surface coverage(θ) were calculated by equation (1).

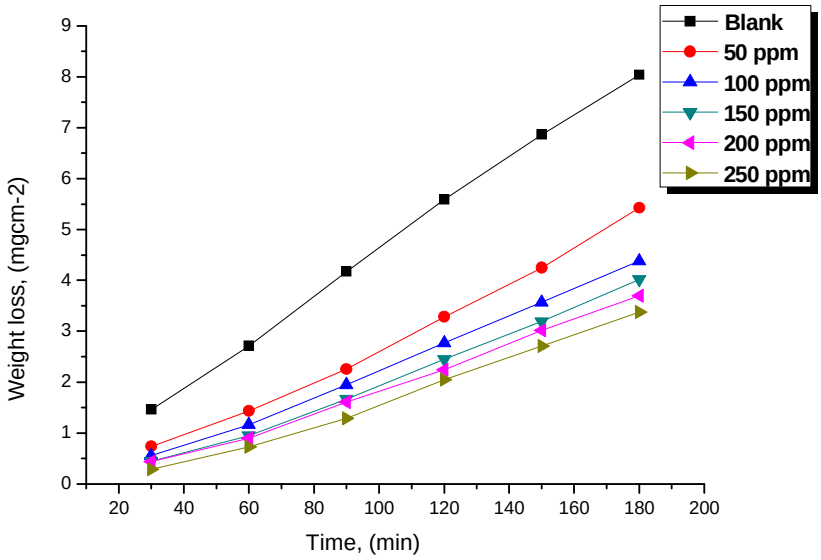

Fig.2: Weight loss-time curves for the corrosion of copper in 1 MHNO_3 in the absence and presence of different concentrations of *Trigonella stellate* extract at 25°C

Table 1: Corrosion rate (C.R.) and inhibition efficiency data obtained from weight loss measurements for copper in 1 M HNO_3 solutions without and with various concentrations of *Trigonella stellate* extract at 25°C

Conc., ppm	Weight loss, mg cm^{-2}	C.R., mg cm^{-2} min^{-1}	θ	%IE
1 M HNO_3	5.587	0.047	……	…….
50	3.283	0.027	0.412	41.2
100	2.768	0.023	0.504	50.4
150	2.450	0.020	0.561	56.1
200	2.244	0.019	0.598	59.8
250	2.048	0.017	0.633	63.3

Table 2: Data of weight loss measurements for copper in 1 M HNO_3 solution in the absence and presence of different concentrations of *Trigonella stellate* at 25–45°C

Conc., ppm	Temp., °C	C.R., mgcm^{-2}min^{-1}	θ	%IE
50	25	0.027	0.412	41.2
	30	0.058	0.333	33.3
	35	0.076	0.255	25.5
	40	0.097	0.186	18.6
	45	0.126	0.095	9.5
100	25	0.023	0.504	50.4
	30	0.048	0.446	44.6
	35	0.064	0.373	37.3
	40	0.080	0.329	32.9
	45	0.105	0.245	24.5
150	25	0.020	00561	56.1
	30	0.043	0.507	50.7
	35	0.057	0.435	43.5
	40	0.072	0.400	40
	45	0.094	0.327	32.7
200	25	0.019	0.598	59.8
	30	0.040	0.548	54.8
	35	0.052	00487	48.7
	40	0.067	0.438	43.8
	45	0.085	0.391	39.1
250	25	0.017	0.633	63.3
	30	0.037	0.574	57.4
	35	0.048	00531	53.1
	40	0.061	0.485	48.5
	45	0.079	0.435	43.5

3.2. Effect of Temperature

The effect of temperature on the corrosion rate of copper in 1M HNO_3 and in presence of different inhibitor concentrations was studied in the temperature range of 298–313K using weight loss measurements.As the temperature increases, the rate of corrosion increases and the inhibition efficiency of the additives decreases as shown in Table2for *Trigonella stellate* extract. The adsorption behavior of inhibitor on copper surface occurs through physical adsorption.

3.3. Adsorption Isotherms

One of the most convenient ways of expressing adsorption quantitatively is by deriving the adsorption isotherm that characterizes the metal/inhibitor/ environment system. Various adsorption isotherms were applied to fit θ values, but the best fit was found to obey Temkin adsorption isotherm which is represented in Figure 3for *Trigonella stellate*,Temkin adsorption isotherm may be expressed by:

$$a\,\Theta = \ln K\,C \qquad (4)$$

Where C is the concentration (ppm) of the inhibitor in the bulk electrolyte, is the degree of surface coverage (Θ=%/100), K ads is the adsorption equilibrium constant. A plot of Θ versus log C should give straight lines with slope equal 2.303/a and the intercept is (2.303/a log K_{ads}). The variation of the adsorption equilibrium constant (K_{ads}) of the inhibitor with their molar concentrations was calculated according to Eq. (2). The experimental data give good curves fitting for the applied adsorption isotherm as the correlation coefficients (R^2) were in the range (0.943-0.999).The equilibrium constant of adsorption K_{ads} obtained from the intercepts of Temkin adsorption isotherm is related to the free energy of adsorption $\Delta G°_{ads}$ as follows:

$$K_{ads} = 1/55.5 \exp\left[-\Delta G°_{ads}\right] / RT \qquad (5)$$

Where, 55.5 is the molar concentration of water in the solution in M^{-1}

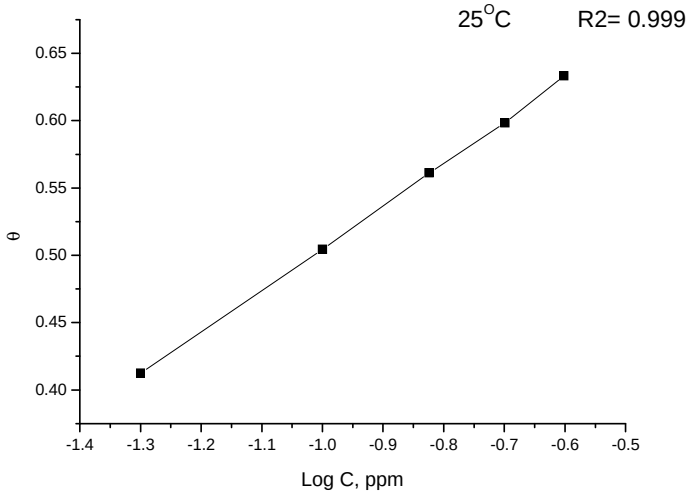

Figure 3: Temkin adsorption isotherm of *Trigonella stellate* on copper surface in 1 M HNO_3 at 25°C

Plots of (ΔG^o_{ads}) versus T Figure 4gave the heat of adsorption (ΔH^o_{ads}) and the standard entropy (ΔS^o_{ads}) according tothe thermodynamic basic equation 6:

$$\Delta G^o_{ads} = \Delta H^o ads - T\,\Delta S^o_{ads} \qquad (6)$$

Table 3clearly shows a good dependence of ΔG^o_{ads} on T, indicating the good correlation among thermodynamic parameters. The negative value of ΔG^o_{ads} ensures the spontaneity of the adsorption process and stability of the adsorbed layer on copper surface. Generally, values of ΔG^o_{ads} around -20 kJ mol^{-1} or lower are consistent with the electrostatic interaction between the charged molecules and the charged metal (physical adsorption).The calculated ΔG^o_{ads} values are closer to -20 kJ mol^{-1} indicating that the adsorption mechanism of the inhibitor on copper in 1 M HNO_3 solutions was typical of physical adsorption. The values of thermodynamic parameters for the adsorption of extract(Table 3)can provide valuable information about the mechanism of corrosion inhibition. While an endothermic adsorption process ($\Delta H^o_{ads} > 0$) is attributed unequivocally to an exothermic adsorption process ($\Delta H^o_{ads} < 0$) may involve either exothermic adsorption or endothermic adsorption or mixture of both processes. In the

presented case, the calculated values of $\Delta H°_{ads}$ for the adsorption of extract in 1 MHNO_3 indicating that *Trigonella stellate* may be physically adsorbed. The ΔS^o_{ads} values in the presence of inhibitor in 1 M HNO_3 are positive. . This indicates that an increase in disorder takes places on going from reactants to the metal-adsorbed reaction complex [17].

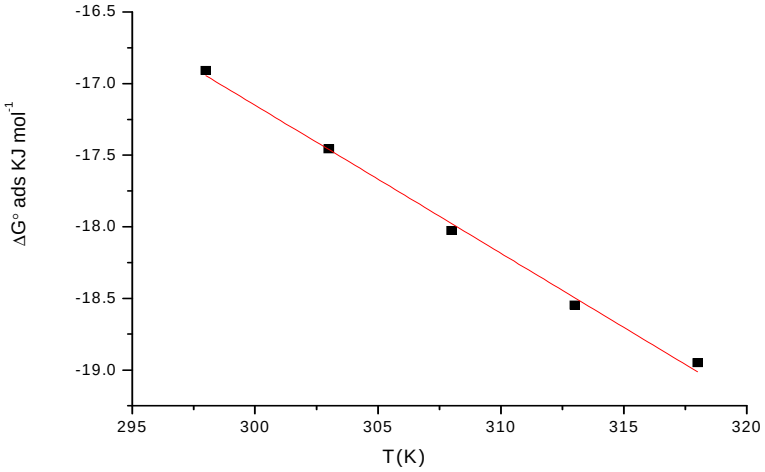

Figure 4: Variation of ΔG^o_{ads} versus T for the adsorption of the inhibitor on copper surface in 1 M HNO_3 at different temperature

Table 3: Thermodynamic parameters for the adsorption of *Trigonella stellate* on copper surface in 1 M HNO_3 at different temperatures

Inhibitor	Temp. °C	K_{ads} M^{-1}	$-\Delta G^o_{ads}$ kJ mol^{-1}	ΔH^o_{ads} kJ mol^{-1}	ΔS^o_{ads} J $mol^{-1}K^{-1}$
Trigonella stellate	25	0.150	16.9	13.9	103.3
	30	0.051	17.5		103.5
	35	2.090	18.0		103.6
	40	0.056	18.5		103.6
	45	0.033	19.5		103.3

3.3 Kinetic –Thermodynamic Corrosion Parameters

The activation parameters for the corrosion process were calculated from Arrhenius-type plot according to eq. (7):

$$k_{corr} = A \exp (E^*_a /RT) \quad (7)$$

Where k_{corr} is the rate of metal dissolution,E^*_a is the apparent activation corrosion energy, R is the universal gas constant, T is the absolute temperature and A is the Arrhenius pre-exponential constant. Values of apparent activation energy of corrosion for copper in 1M HNO_3without and with various concentrations of *Trigonella stellate* were determined from the slope of log (k_{corr}) versus 1/T plots and are shown in Figure 5. The alternative formulation of transition state equation is shown in Eq. (8):

$$k_{corr} = (RT/Nh) \exp (\Delta S^*/R)\exp (-\Delta H^*/RT) \quad (8)$$

Where h is Planck's constant, N is Avogadro's number, ΔS^* is the entropy of activation and ΔH^* is the enthalpy of activation.Figure 6shows a plot of log k against (1/T) in 1 M HNO_3. Straight lines are obtained with slopes equal to (ΔH^*/2.303R) and intercepts log (R/Nh + ΔS^*/2.303R), their values are recorded in Table 4.The increase in E_a^* with increase inextract concentration (Table 4)is typical of physical adsorption. The positive signs of the enthalpies (ΔH^*) reflect the endothermic nature of the copper dissolution process. Value of entropies (ΔS^*) imply that the activated complex at the rate determining step represents an association rather than a dissociation step, meaning that a decrease in disordering takes place on going from reactants to the activated complex [18,19].

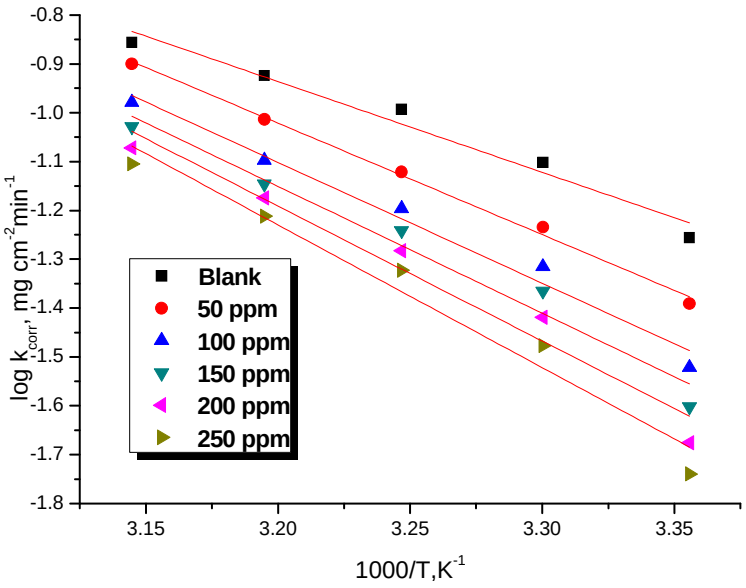

Figure 5: Log k_{corr} vs. (1/T) curves for Arrhenius plots for copper corrosion rates after 120 minute of immersion in 1M HNO_3 in the absence and presence of various concentrations of *Trigonella stellate* extract

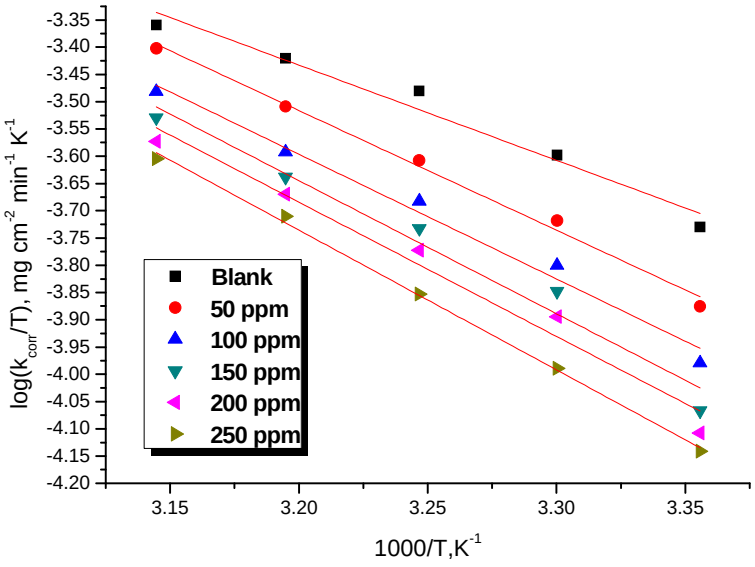

Figure 6: Log (k_{corr}/T) vs. (1/T) curves for Transition plots for copper corrosion rates after 120 minute of immersion in 1M HNO_3 in the absence and presence of various concentrations of *Trigonella stellate*

Table 4: Activation parameters for copper corrosion in the absence and presence of various concentrations of *Trigonella stellate* extract in 1M HNO_3

Conc. ppm	E_a^*, kJ mol^{-1}	ΔH^*, kJ mol^{-1}	$-\Delta S^*$, J mol^{-1} K^{-1}
1 M HNO_3	35.6	14.5	156.3
50	43.7	18.2	130.5
100	47.4	19.0	126.3
150	49.7	20.3	117.7
200	52.9	20.5	117.3
250	55.9	21.3	112.0

3.5 PolarizationTests

Figure 7 shows potentiodynamic polarization curves recorded for copper in 1 M HNO_3 solutions in the absence and presence of various concentrations of *Trigonella stellate* extract at 25ºC. The presence of *Trigonella stellate* extract shifts both anodic and cathodic branches to the lower values of corrosion current densities and thus causes a remarkable decrease in the corrosion rate. The parameters derived from the polarization curves are given in Table 5. In 1 M HNO_3 solution, the presence of *Trigonella stellate* extract causes a remarkable decrease in the corrosion rate i.e., shifts both anodic and cathodic curves to lower current densities. In other words, both cathodic and anodic reactions of copper electrode are retarded by *Trigonella stellate* in 1 M HNO_3 solution. The Tafel slopes of β_a and β_c at 25ºC do not change remarkably upon addition of the inhibitor, which indicates that the presence of *Trigonella stellate* extract does not change the mechanism of hydrogen evolution and the metal dissolution process. Generally, an inhibitor can be classified as cathodic type if the shift of corrosion potential in the presence of the inhibitor is more than 85 mV with respect to that in the absence of the inhibitor [20,21]. In the presence of *Trigonella stellate*, E_{corr} shifts to less negative but this shift is very small (about 20-30 mV), which indicates that *Trigonella stellate* extract can be arranged as mixed type inhibitor. Since βc> βa, *Trigonella stellate* extract can be classified as mixed type inhibitor but the cathode is more polarized than the anode when an external current was applied.

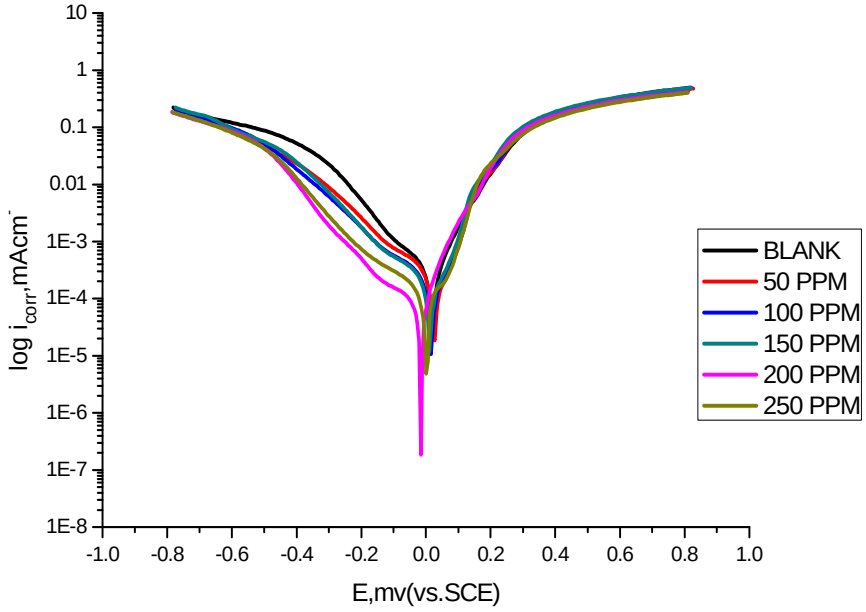

Figure 7: Potentiodynamic polarization curves for the corrosion of copper in 1 M HNO_3 solution without and with various concentrations of *Trigonella stellate* at 25˚C

Table 5: Effect of concentration of *Trigonella stellate* on the electrochemical parameters calculated using potentiodynamic polarization technique for the corrosion of copper in 1 M HNO_3 at 25˚C

Conc. , ppm	i_{corr}, µA cm^{-2}	$-E_{corr}$, mV vs. SCE	β_a, $mVdec^{-1}$	β_c, $mVdec^{-1}$	CR, mm y^{-1}	θ	%IE
1 M HNO_3	267	19.6	100.1	173	266	----	-----
50	169	26.3	87.3	190.	163	0.388	38.8
100	126	18.3	84.8	188.9	121	0.543	54.3
150	125	13.1	81.2	179.2	120	0.547	54.7
200	82.3	15.6	117.8	204.1	79.3	0.702	70.2
250	60.9	843	81.7	177.1	58.7	0.779	77.9

3.6 Electrochemical Impedance Spectroscopy (EIS) Tests

EIS is well-established and it is powerful technique for studying the corrosion. Surface properties, electrode kinetics and mechanistic information can be obtained from impedance diagrams (22-26).Figure8shows the Nyquist (a) and Bode (b) plots obtained at open-circuit potential both in the absence and presence of increasing concentrations of *Trigonella stellate* at 25°C. The increase in the size of the capacitive loop with the addition of *Trigonella stellate*extract shows that a barrier gradually forms on the copper surface. The increase in the capacitive loop size (Figure 8a)increase by increasing inhibitor concentration.. Bode plots (Figure 8b), show that the total impedance increases with increasing inhibitor concentration (log Z vs. log f). But (log f vs. phase), also Bode plot shows the

continuous increase in the phase angle shift, obviously correlating with the increase of inhibitor adsorbed on copper surface. The Nyquist plots do not yield perfect semicircles as expected from the theory of EIS. The deviation from ideal semicircle was generally attributed to the frequency dispersion [27]as well as to the inhomogeneity of the surface.

EIS spectra of the investigated compound were analyzed using the equivalent circuit, Figure 9, which represents a single charge transfer reaction and fits well with our experimental results. The constant phase element, CPE, is introduced in the circuit instead of a pure double layer capacitor to give a more accurate fit [28].The double layer capacitance, C_{dl}, for a circuit including a CPE parameter (Y_0 and n) were calculated from eq.9[29]:

$$C_{dl} = Y_0 (\omega_{max})^{n-1} \quad (9)$$

where Y0 is the magnitude of the CPE, $\omega_{max} = 2\pi f_{max}$, f_{max} is the frequency at which the imaginary component of the impedance is maximal and the factor n is an adjustable parameter that usually lies between 0.50 and 1.0. After analyzing the shape of the Nyquist plots, it is concluded that the curves approximated by a single capacitive semicircles, showing that the corrosion process was mainly charged-transfer controlled [30,31].The general shape of the curves is very similar for all samples (in presence or absence of inhibitor at different immersion times) indicating that no change in the corrosion mechanism [32].From the impedance data Table 6,we concluded that the value of R_{ct} increases with increasing the concentration of the inhibitor and this indicates an increase in % IE_{EIS}, which in concord with the EFM results obtained. In fact, the presence of inhibitors enhances the value of R_{ct} in acidic solution. Values of double layer capacitance are also brought down to the maximum extent in the presence of inhibitor and the decrease in the values of CPE follows the order similar to that obtained for i_{corr} in this study. The decrease in CPE/C_{dl} results from a decrease in local dielectric constant and/or an increase in the thickness of the double layer, suggesting that organic derivatives inhibit the copper corrosion by adsorption at metal/acid [33, 34] .The inhibition efficiency was calculated from the charge transfer resistance data from eq.10[35]:

$$\% IE_{EIS} = [1 - (R^{\circ}_{ct} / R_{ct})] \times 100 \quad (10)$$

Where Ro ct and R_{ct} are the charge-transfer resistance values without and with inhibitor respectively.

Table 6: Electrochemical kinetic parameters obtained by EIS technique for copper in 1 M HNO_3 without and with various concentrations of *Trigonella stellate* extract at 25ºC

Conc., ppm,	R_{ct}, Ω cm^2	C_{dl}, µF cm^{-2}	θ	%IE
1.0 M HNO_3	123.0	780	-----	------
50	190.2	430	0.353	35.3
100	630.6	360	0.805	80.5
150	711.8	310	0.827	82.7
200	966.6	307	0.873	87.3
250	1276.0	230	0.904	90.4

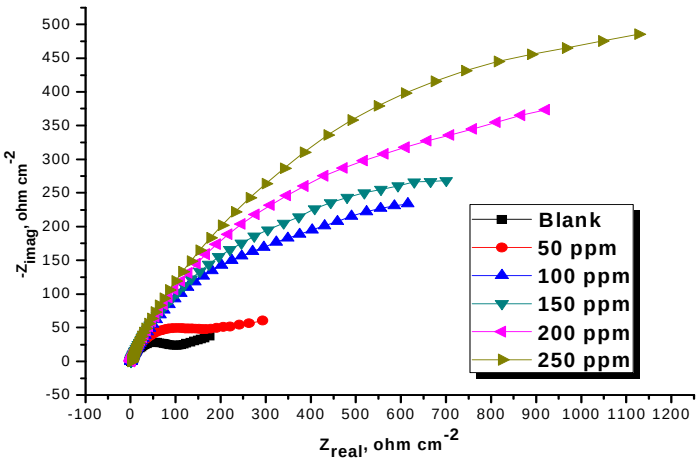

Figure 9a: The Nyquist plots for the corrosion of copper in 1M HNO_3 in the absence and presence of different concentrations of *Trigonella stellate* at 25ºC

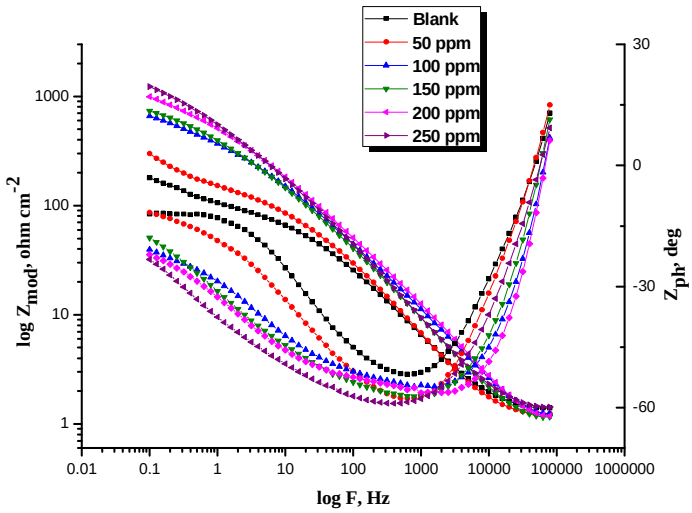

Figure 9 b: The Bode plots for the corrosion of copper in 1M HNO_3 in the absence and presence of different concentrations of *Trigonella stellate* at25ºC

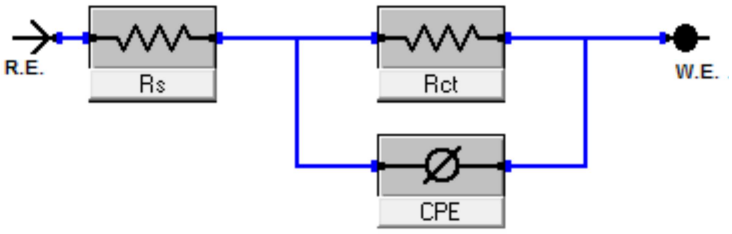

Figure 9: Equivalent circuit model used to fit experimental EIS

3.7Electrochemical Frequency Modulation (EFM) Tests

EFM is a nondestructive corrosion measurement technique that can directly and quickly determine the corrosion current values without prior knowledge of Tafel slopes, and with only a small polarizing signal. These advantages of EFM technique make it an ideal candidate for online corrosion monitoring [36].The great strength of the EFM isthe causality factors which serve as an internal check on the validity of EFM measurement. The causality factors CF-2 and CF-3 are calculated from the frequency spectrum of the current responses.Figure 10shows the EFM Intermodulation spectra (current vs frequency) of copper in HNO_3 solution containing different concentrations of *Trigonella stellate*. The larger peaks were used to calculate the corrosion current density (i_{corr}), the Tafel slopes (β_c and β_a) and the causality factors (CF-2 and CF-3).These electrochemical parameters were listed in Table 7.The data presented in Table 7obviously show that, the addition of *Trigonella stellate* at a given concentration to the acidic solution decreases the corrosion current density, indicating that this compound inhibits the corrosion of copper in 1M HNO_3 through adsorption. The causality factors obtained under different experimental conditions are approximately equal to the theoretical values (2 and 3) indicating that the measured data are verified and of good quality. The inhibition efficiencies $\%IE_{EFM}$ increase by increasing the inhibitor concentrations and was calculated as from Eq. (11):

$$\%IE_{EFM} = [1-(i_{corr}/i^{o}_{corr})] \times 100 \qquad (11)$$

Where i^{o}_{corr} and icorr are corrosion current densities in the absence and presence of *Trigonella stellate*

Table 7: Electrochemical kinetic parameters obtained from EFM technique for copper in 1M HNO_3 in the absence and presence of different concentrations of *Trigonella stellate* extract at 25ºC

Conc., Ppm	i_{corr}, μAcm^{-2}	β_a mV dec^{-1}	β_c mV dec^{-1}	C.R. mpy	CF-2	CF-3	θ	%IE
1M HNO_3	127.5	0.072	138	122.9	1.812	2.667	…..	…..
50	64.87	0.058	137	62.53	1.829	2.518	0.491	49.1
100	42.76	0.057	295	41.22	1.827	3.241	0.665	66.5
150	32.29	0.0509	218	31.12	1.834	2.957	0.747	74.7
200	25.31	0.052	218	24.39	1.836	3.071	0.802	80.2
250	19.62	0.0504	196	18.91	1.788	2.875	0.846	84.6

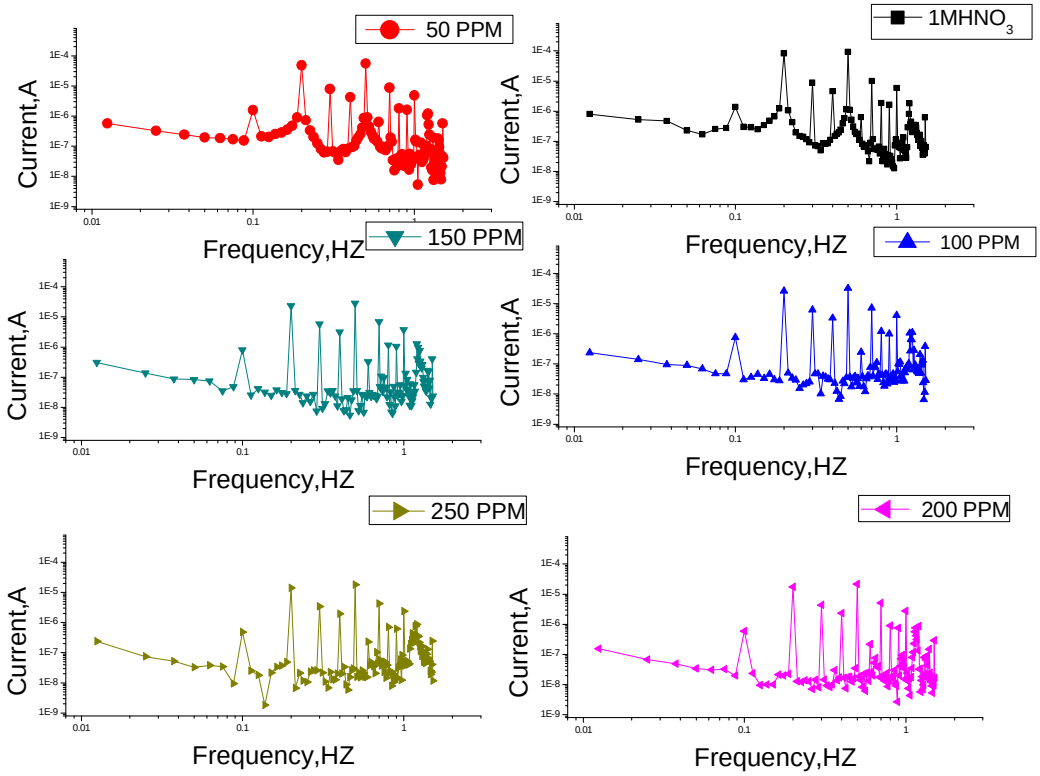

Figure 10: EFM spectra for copper in 1 M HNO_3 in the absence and presence of different concentrations of *Trigonella stellate* at 25ºC

3.8Surface Morphology

In order to verify if the *Trigonella stellate* molecules are in fact adsorbed on copper surface, scanning electron microscope (SEM) experiments were carried out. The SEM micrographs for copper surface alone and after 24 h immersion in 1 M HNO_3 without and with the addition of 250 ppm are shown in Figures (11a-c). As expected, Figure11ashows metallic surface is clear, while in the absence of *Trigonella stellate*, the copper surface is damaged by HNO_3corrosion (Figure11b). In contrast, in presence of the investigated compound (Figures 11c); the metallic surface seems to be almost no affected by corrosion. The formation of a thin film of *Trigonella stellate* observed in SEM micrograph, thus protecting the surface against corrosion.

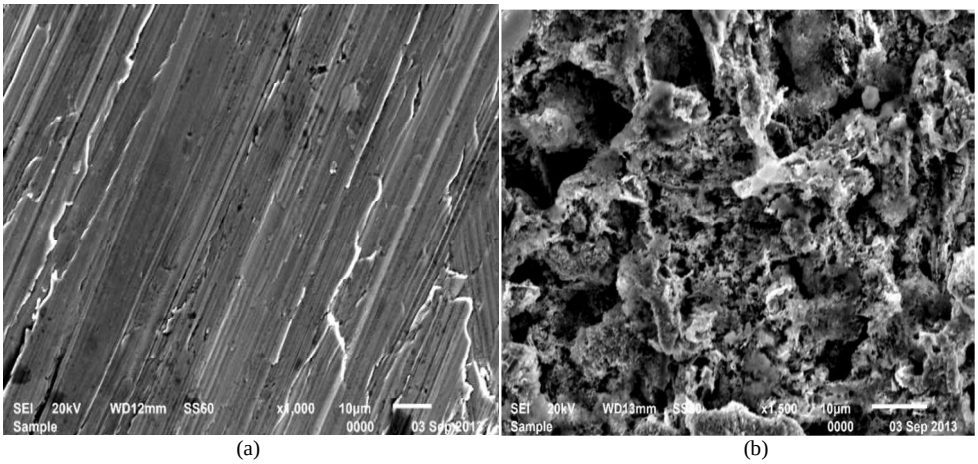

(a) (b)

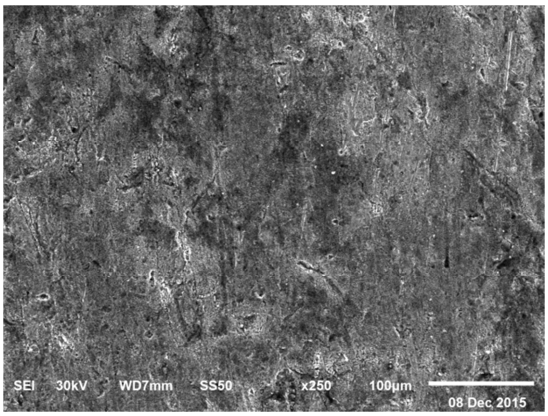

(c)

Figure 11: SEM micrographs of copper surface (a) before of immersion in 1 M HNO_3, (b) after 24 h of immersion in 1 M HNO_3, (c) after 24 h of immersion in 1 M HNO_3+ 250 ppm Trigonela stellate extract at 25°C

3.9 Mechanism of Corrosion Inhibition

In acidic solutions, transition of the metal/solution interface is attributed to the adsorption of the inhibitor molecules at the metal/solution interface, forming a protective film. The rate of adsorption is usually rapid, and hence, the reactive metal surface is shielded from the acid solutions [49]. The adsorption of an inhibitor depends on its chemical structure, its molecularsize, the nature and charged surface of the metal, anddistribution of charge over the whole inhibitor molecule. Infact, adsorption process can occur through the replacementof solvent molecules from the metal surface by ions andmolecules accumulated near the metal/solution interface.Ions can accumulate at the metal/solution interface in excessof those required to balance the charge on the metal at the operating potential. These ions replace solvent molecules from the metal surface, and their centers reside at the inner Helmholtz plane. This phenomenon is termed specific adsorption, contact adsorption. The anions are adsorbed when the metal surface has an excess positive charge in an amount greater than that required to balance the charge corresponding to the applied potential. The exact nature of the interactions between a metal surface and an aromatic molecule depends on the relative coordinating strength towards the given metal of the particular groups present [37]. Generally, two modes of adsorption were considered. In one mode, the neutral molecules of extract can be adsorbed on the surface of copper through the chemisorption mechanism, involving the displacement of water molecules from the copper surface and the sharing electrons between the heteroatoms and Cu. The inhibitor molecules can also adsorb on the Cu surface based on donor-acceptor interactions between π-electrons of the aromatic/heterocyclic ring and vacant d-orbitals of surface Cu. In another mode, since it is well known that the Cu surface bears the positive charge in acidic solutions [38], so it is difficult for the protonated extract to approach the positively charged Cu surface (H_3O^+/metal interface) due to the electrostatic repulsion. Since chloride ions have a smaller degree of hydration, thus they could bring excess negative charges near the interface and favors more adsorption of the positively charged inhibitor molecules, the protonated extract adsorbed through electrostatic interactions between the positively charged molecules and the negatively charged metal surface. . According to Ben abdellah *et al* [38], synergistic intermolecular effects of the active molecules of Trigonela stellate extract adsorbing on the corroding surface, as well as its cathodic inhibitory effect, which could modify the hydrogen reduction, are responsible for its efficiency as a corrosion inhibitor.

CONCLUSION

Trigonella stellate extractwas good corrosion inhibitor for copper in 1 M HNO_3 solution.Reasonably good agreement was observed between the values obtained by the weight loss and electrochemical measurements.Results obtained from potentiodynamic polarization indicated that Trigonela stellate is mixed-type inhibitor.Percentage inhibition efficiency of *Trigonella stellate* was temperature dependent and its addition led to a increase of the activation corrosion energy. The thermodynamic parameters revealed that the inhibition of corrosion by *Trigonella stellate* extract is due to theformation of a physical adsorbed film on the metal surface.The adsorption of *Trigonella stellate* onto copper surface follows the Temkin adsorption isotherm model.The negative values of the free energy of adsorption and adsorption heat are indicating that the process was spontaneous and endothermic.

REFERENCES

[1] KFKhaled, *Electrochim. Acta*,**2009,** 54: 4345-4352.
[2] TKosec, DKMerl, IMilošev, *Corros. Sci.*, **2008,** 50: 1987-1997.
[3] **K** Rahmouni, NHajjaji, MKeddam, ASrhiri, HTakenouti, *Electrochim. Acta*, **2007,** 52: 7519-7528.
[4] DNSingh,AKDey, *Corrosion*,**1993,** 49: 594-600.
[5] GBanerjee, SNMalhotra, *Corrosion*,**1992,** 48: 10-15.

[6] STArab, EANoor, *Corrosion*,**1993,** 49: 122-129.
[7] IARaspini, *Corrosion*, **1993,** 49: 821-828.
[8] RFVVillamil., PCorio, JCRubim, ASiliva, MLgostinho, *J. Electroanal. Chem.*, **1999,** 472:112-118.
[9] KSParikh,KJJoshi, *Trans. SAEST*, **2004,** 39: 29-35.
[10] JSChauhan, *Asian Journal of Chemistry*, **2009,** 21: 1975-1978.
[11] TVSangeetha,MFredimoses, *E-Journal of Chemistry*, **2011,** 8: (S1), S1-S6.
[12] Fernando Sílvio de Souza, Cristiano Giacomelli, ReinaldoSimõesGonçalves, AlmirSpinelli**.,** *Materials Science and Engineering*,**2012,** 32: 2436-2444.
[13] BAAbd-El-Nabey, AMAbdel-Gaber, MElSaid Ali, EKhamis,S El-Housseiny, *J. Electrochem. Sci.*,**2013,** 8: 5851-5865.
[14] GNMu, TPZhao, MLiu, TGu, *Corrosion*,**1996,** 52: 853-856.
[15] RGParr, RADonnelly, MLevy, WEPalke, *J. Chem. Phys.*, **1978,** 68, 3801-3807**.**
[16] RWBosch, JHubrecht, WFBogaerts, BCSyrett, *Corrosion*,**2001,**57, 60-70.
[17] G Banerjee,SNMalhotra, *Corrosion*.**1992,** 48, 10-15
[18] Hour T P & Holliday R D**,** *Journal of Metallurgy*.**1953**,3, 502-510
[19] LO Riggs Jr., TJ Hurd, *Corrosion*, **1967,** 23(8), 252–260
[20] GM Schmid, HJ Huang, *Corros. Sci*.**1980,** 20(8-9), 1041–1057,
[21] Bentiss F. Lebrini M. and Lagrenee M., *Corros. Sci*., **2005,** 47, 2915–2931.
[22] Marsh J, Advanced Organic Chemistry, 3rd edn (Wieley Eastern, New Delhi), *J. Metallurgy*, **1988,** 2012 , 13-26**.**
[23] HPLee,KNobe., *J. Electrochem. Soc.* **1986,** 133: 2035- 2043.
[24] ZHTao, STZhang, WHLi, BRHou, *Corros. Sci*.**2009,** 51: 2588-2595.
[25] ESFerreira, CGiacomelli, FCGiacomelli, ASpinelli, *Mater. Chem.Phys*.**2004,** 83: 129-134.
[26] DCSilverman,JECarrico, *Corrosion*.**1988,** 44, 280-289
[27] WJLorenz,FMansfeld, *Corros.Sci.***1981,** 21, 647-653
[28] DDMacdonald, MCMckubre, "Impedance measurements in Electrochemical systems," Modern Aspects of Electrochemistry, J.O'M. Bockris, B.E. Conway, R.E.White, Eds., Plenum Press, New York, New York, **1982**,1461
[29] FMansfeld; *Corrosion.***1981,** 36, 301-310
[30] CGabrielli,"Identification of Electrochemical processes by Frequency Response Analysis,"Solarton Instrumentation Group, **1980.**
[31] MEl Achouri, SKertit, HMGouttaya, BNciri, YBensouda, LPerez, MRInfante, KElkacemi, *Prog. Org. Coat*.**2001**, 43, 267-273
[32] JRMacdonald, WBJohanson, in: JR Macdonald (Ed.), Theory in Impedance Spectroscopy, John Wiley& Sons, New York, **1987**.
[33] SFMertens, CXhoffer, BCDecooman, E. Temmerman, *Corrosion*.**1997**, 53, 381-388
[34] GTrabanelli,CMontecelli, VGrassi, AFrignani, *J. Cem. Concr., Res*.**2005**, 35, 1804-1809 .
[35] AJTrowsdate, BNoble, SJHaris, ISRGibbins, GEThomson, GCWood, *Corros. Sci*.**1996**, 38, 177-182
[36] FMReis, HG De Melo,ICosta, *Electrochim. Acta.* ***2006,*** 51, 17-23
[37] MLagrenee, BMernari, MBouanis, MTraisnel,FBentiss, *Corros. Sci.***2002**, 44, 573-579
[38] M Benabdellah, M Benkaddour, B Hammouti, M Bendahhou, A Aouniti: *Appl. Surf. Sci.*, **2006**, 252, 6212–6217.